

**Cell Reports Methods, Volume 1**

**Supplemental information**

**KiRNet: Kinase-centered network**

**propagation of pharmacological screen results**

**Thomas Bello, Marina Chan, Martin Golkowski, Andrew G. Xue, Nithisha Khasnavis, Michele Ceribelli, Shao-En Ong, Craig J. Thomas, and Taranjit S. Gujral**

## **Supplemental information**

KiRNet: Kinase-centered network propagation of pharmacological screen results

Thomas Bello, Marina Chan, Martin Golkowski, Andrew G. Xue, Nithisha Khasnavis, Michele Ceribelli, Shao-En Ong, Craig Thomas, and Taranjit S. Gujral

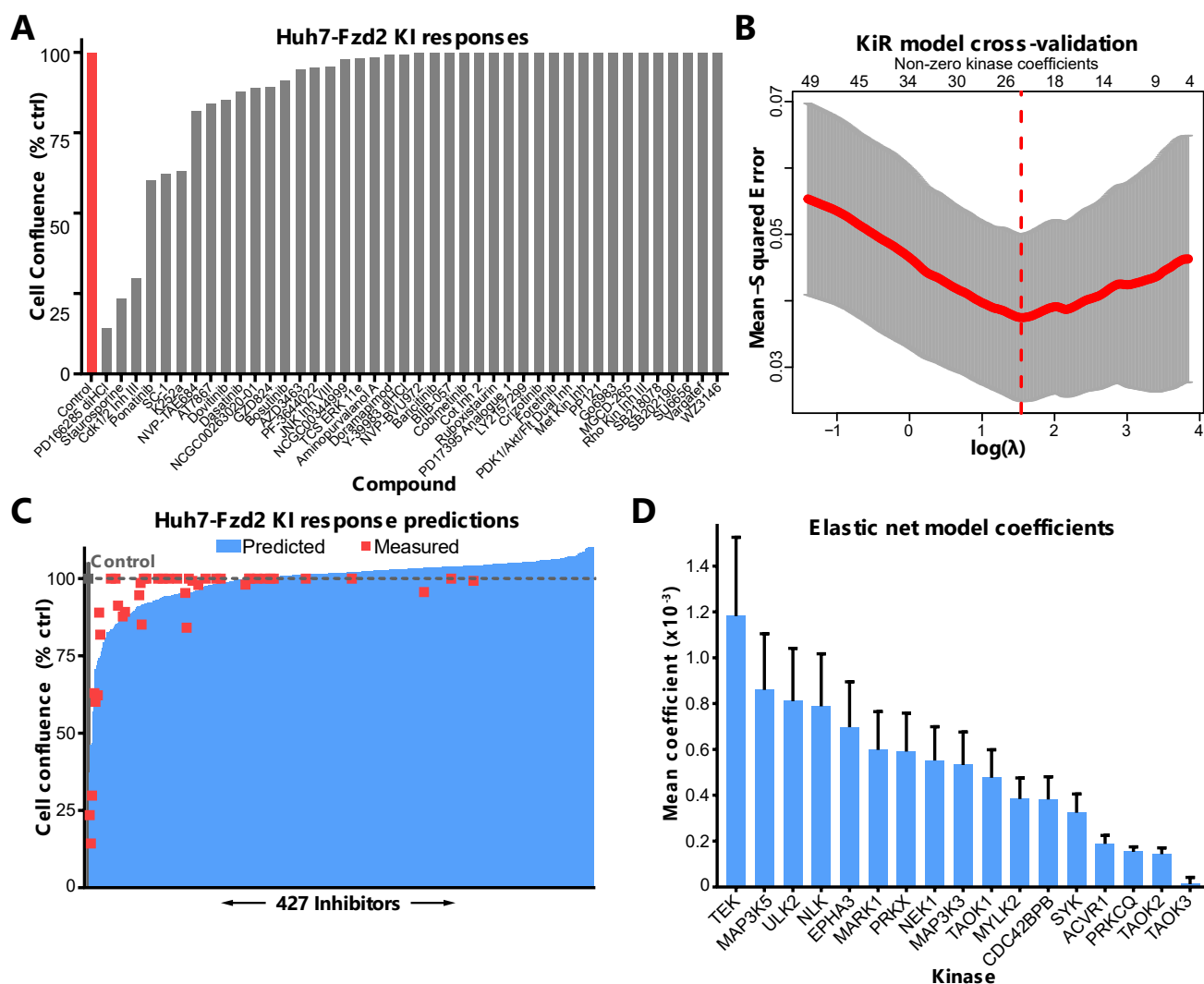
### **SUPPLEMENTARY INFORMATION**

Figure S1. Generation of Huh7-Fzd2 KiR model, related to Figure 1

Figure S2. Validation of final KiRNet high-value model, related to Figures 1 and 2

Data S1. List of key kinases, Huh7-Fzd2 refined and high-value subnetwork nodes and properties, related Figure 1

Data S2. Small molecule inhibitors, qPCR primers, and siRNA sequences used (extension of Key Resources Table), related Figure 2



**Figure S1. Generation of Huh7-Fzd2 KiR model, related to Figure 1. (A)** Interpolated cellular confluence responses of Huh7-Fzd2 cells to 42 KIs (plus control). Cells were treated with 7 doses of each KI, and their endpoint cellular confluence was quantified as the response. These responses were fit with a sigmoidal Hill equation and interpolated at the dose at which the compound was profiled (usually 500nM). Data presented as % of untreated control. **(B)** Cross validation curve for the elastic net KiR model demonstrating the selection of the optimal penalty scalar  $\lambda$ . Models were computed for 300 geometrically distributed values of  $\lambda$  and evaluated via leave-one-out cross validation (LOOCV). Horizontal axis displays the logarithm of  $\lambda$ , vertical axis displays the LOOCV mean-square error  $\pm$  standard deviation. The value of  $\lambda$  for which this error reaches a minimum, indicated by the red dotted line, is chosen for the final model. **(C)** KiR model predictions for Huh7-Fzd2 response to all KIs profiled. Horizontal axis displays 427 KIs, vertical axis displays the response to that KI. Red dots represent experimentally measured values used to build the model, blue bars represent the KiR model predicted response to each KI. **(D)** Elastic net coefficients for the kinases selected as key functional nodes for Huh7-Fzd2 cell proliferation. Data presented as mean  $\pm$  standard deviation for the coefficients across 10 values of the elastic net hyperparameter  $\alpha$ .

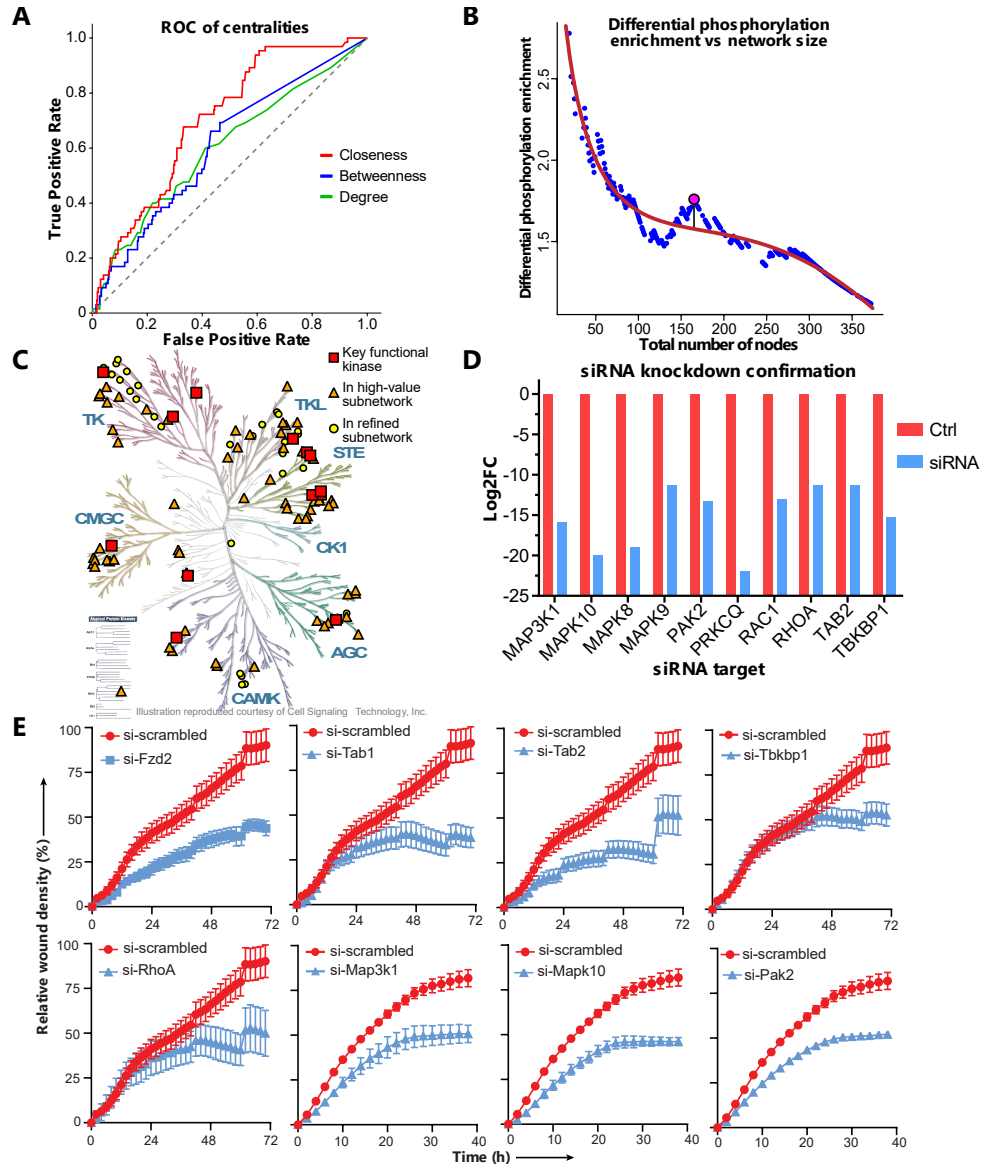


**Figure S2. Validation of final KiRNet high-value model, related to Figures 1 and 2.** (A) Receiver-operator characteristic curves for three centrality measures and their ability to identify differentially phosphorylated nodes. Closeness, defined as the inverse of the average distance from a given node to all other nodes in the network, outperforms both degree (the number of edges connected to a node) and betweenness (the fraction of all shortest paths between all pairs of nodes that pass through a given node). (B) Plot of the enrichment of differentially phosphorylated nodes versus the size (total number of nodes) of the high-value network, for each empirically tested cutoff for refined closeness. Data was fit with a third-degree polynomial model of the square root of the size ( $R^2 = 0.947$ ). Pink point represents the point with the maximum residual that was chosen for the final model, to maximize enrichment while minimizing the size (relative to the fitted relationship). (C) KinMap of kinases predicted by KiR and KiRNet to be important for Huh7-Fzd2 cell proliferation. Red squares are KiR predicted kinases, orange triangles are kinases present in the high-value subset, and yellow circles are kinases present in the optimally refined subnetwork. (D) Confirmation of siRNA knockdown for select genes. Data was normalized using the  $2^{-\Delta\Delta Ct}$  method, normalized to GAPDH. (E) Time-course plots of wound-healing assay. Huh7-Fzd2 cells were transfected with transient siRNA knockdowns of the indicated high-value gene targets. Data presented as mean  $\pm$  SEM of three biological replicates.